Available online at www.sciencedirect.com
ScienceDirect
Cement and Concrete Research 36 (2006) 1931–1938
Cement and Concrete Research

Bond behaviour of corroded reinforcing steel bars in concrete

Congqi Fang [a,*], Karin Lundgren [b], Mario Plos [b], Kent Gylltoft [b]

[a] Department of Civil Engineering, Shanghai Jiaotong University, Shanghai 200240, China
[b] Department of Civil and Environmental Engineering, Structural Engineering, Chalmers University of Technology, SE-412 96, Göteborg, Sweden

Received 29 July 2005; accepted 16 May 2006

Abstract

The effect of steel corrosion on bond between steel bars and the surrounding concrete was investigated for different corrosion levels. Both pullout tests and finite element analysis were used and the results from the two were compared. An electrolyte corrosion technique was used to accelerate steel corrosion. For confined deformed bars, a medium level (around 4%) of corrosion had no substantial influence on the bond strength, but substantial reduction in bond took place when corrosion increased thereafter to a higher level of around 6%. It is demonstrated that the confinement supplied an effective way to counteract bond loss for corroded steel bars of a medium (around 4% to 6%) corrosion level. The results of finite element analyses, where it was assumed that rust behaved like a granular material, showed a reasonably good agreement with the experiments regarding bond strength and bond stiffness.

Keywords: Bond strength; Reinforcement; Corrosion; Reinforced concrete

1. Introduction

As the interaction between reinforcing steel and the surrounding concrete, bond is fundamental for all reinforced concrete structures. For those concrete structures located in an aggressive environment bond may be weakened by corrosion of the reinforcing steel, affecting the serviceability and ultimate strength of concrete elements within the structure. While some researchers think corrosion of a limited degree improves the bond between steel and concrete [1], corrosion is considered one of the main causes for the limited durability of steel-reinforced concrete [2]. The basic problem associated with the deterioration of reinforced concrete due to corrosion is not that the reinforcing steel itself is reduced in mechanical strength, but rather that the corrosion products due to the volume increase cause splitting [3]. Studies conducted by Auyeung confirmed that the loss of bond strength for an unconfined corroded reinforcing steel bar is much more critical than the cross section loss, since a 2% diameter loss could lead to 80% bond reduction [4].

The interaction of reinforcing steel bars with concrete is a complex phenomenon that has important effects on the response characteristics of reinforced concrete elements and structures. A large number of research programmes have been carried out in the area of steel–concrete bond behaviour, such as those by Tepfers [5,6]. Also, many researchers have conducted studies on the mechanism of bond failure. For example, Cairns and Jones proposed an analysis of the bond strength of ribbed reinforcing bars in which bond failure was considered as bearing failure of the ribs on the concrete. Cairns and Jones's analysis suggested that bond strength was only partially dependent on the splitting resistance of the beam section [7,8]; Balázs developed a theory for crack formation in reinforced concrete based on an analysis of slip, bond stresses and steel stresses, and steel stress was presented. The problem was treated as an initial value problem both for initial crack formation when the cracks were independent, and for stabilized crack formation when the cracks were independent, and for stabilized crack formation when the zones of bond stresses reached each other [9].

The deterioration in bond is of particular concern for concrete structures when the embedded steel reinforcing bars are corroded. Many studies have been conducted on the influence of corrosion on bond between steel and concrete [3,4,10–20]. Due

* Corresponding author. Tel./fax: +86 21 54744558.
E-mail address: cqfang@sjtu.edu.cn (C. Fang).

0008-8846/$ - see front matter © 2006 Elsevier Ltd. All rights reserved.
doi:10.1016/j.cemconres.2006.05.008

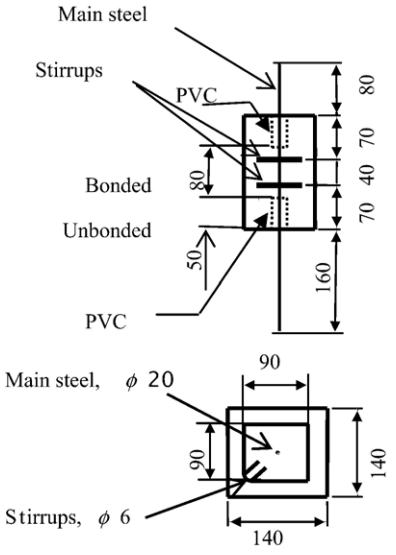

Fig. 1. Specimen geometry. All dimensions in mm.

to the nonuniformity in bond stress, experiments have been the primary method for studying how corrosion affects the bond mechanism. Experiments provide a simple, effective way of evaluating the effects of different parameters on bond behaviour. However, due to the difficulty of obtaining the exact expected levels of reinforcement corrosion from experiments, numerical modeling is becoming increasingly important as an alternative or supplementary method for studying the effect of corrosion on bond behaviour [21–24]. A disadvantage of this approach is that a bond–slip relation is predefined and some circumstances have to be known in advance, including whether the concrete will split or the reinforcement will yield [25].

In this study the effect of reinforcement corrosion on bond is investigated using comparisons between the results of analysis and those from the tests carried out. The research program was conducted for reinforcing bars of different corrosion levels. Specimens were first investigated under pullout loads, and were then modelled with nonlinear finite element analysis.

2. Experiment

A total of 24 pullout specimens were included within the current investigation. The test specimens were divided into two major groups: Confined and unconfined specimens. Each major group was divided into 4 small groups according to the target steel corrosion from 0% (non-corrosion) to 6%. Three replicate specimens were cast within each small group.

Hot-rolled deformed steel bars, 20 mm in diameter and 420 mm in length, were used as the main reinforcing steel in all specimens. The embedment length was four times the bar diameter, e.g., 80 mm, as shown in Fig. 1. For those specimens with stirrups supplying lateral confinement, round steel with a diameter of 6 mm was selected for rectangular closed stirrups with a spacing of 40 mm, as shown in Fig. 1, which shows the geometry of the specimens. The main reinforcing steel had a yield point of 351 MPa and a tensile strength of 521 MPa.

The concrete cast had a target compressive strength of 50 to 55 MPa. Ordinary (ASTM C150 Type I) Portland cement, fine aggregate (medium sized natural sand), and coarse aggregate (crushed limestone) in the ratio of cement/sand/coarse aggregate = 410 : 658 : 1120 at a water/cement ratio of 0.44 were used to prepare the concrete mixture. Concrete cubes with dimensions of $100 \times 100 \times 100$ mm^3 were also cast for the concrete compressive strength. After casting, the concrete specimens, both test specimens and cubes for compressive strength, were kept in the moulds and cover with damp polyethylene for 3 days. They were then demoulded and kept in a curing room maintained at 20 ± 3 °C and 90% or greater relative humidity. The 28-day cured specimens had an average measured strength of 52.1 MPa.

An electrolyte corrosion technique was used to accelerate steel corrosion. The 28-day cured specimens were fully immersed in a 5% NaCl solution in a plastic tank. Electric current and the duration of exposure were used for the theoretically estimated mass loss of reinforcing steel due to corrosion according to Faraday's Law. Power supplies with adjustable voltage and direct current (from 0 to 2 A) were chosen for the electrolyte corrosion process. The direct current was impressed on the main steel bar embedded in the concrete, using an integrated system incorporating a rectifier with a built-in ammeter to monitor the current, and a potentiometer to control the current intensity. The direction of the electric current was such that the reinforced steel bar served as the anode while a stainless steel plate counter-electrode was positioned in the tank to act as a cathode. The stainless steel plate that served as the cathode consumed the excess electrons given off by the reinforcement during the corrosion process. The theoretically estimated mass loss of steel due to corrosion can be expressed by the following equation [4]:

$$m_t = \frac{T \times \bar{I} \times 55.847}{2 \times 96487} \quad (1)$$

where T is the duration of exposure and $\bar{I}$ the average magnitude of electrical current.

Eq. (1) is based on Faraday's Law, which states: (1) The mass of substance formed or consumed in electrolysis is proportional to the amount of charge passing through it; (2) The mass of a substance formed or consumed in electrolysis is also proportional to its molar mass; (3) The mass of a substance formed or consumed in electrolysis is inversely proportional to number of electrons per mole needed to cause the indicated change in the oxidation state. The quantity of applied charge of any electrolysis is given by the product of applied current and the duration of exposure. For the corrosion process, for each mole of iron oxidized, 2 mol of electrons are given out, consuming a charge of 2×96487 coulombs (C). The mass loss is then calculated by multiplying the applied charge by the molar mass (55.847 g/mol for iron) and dividing by charge needed per mole. This technique was successfully adopted by many researchers [4,10].

The mass loss of reinforcing steel due to corrosion was used to select the density of electric current and the duration of exposure according to Eq. (1). The actual degree of corrosion, or corrosion level was, however, measured as the loss in weight of the steel bar relative to the weight of the bond length before

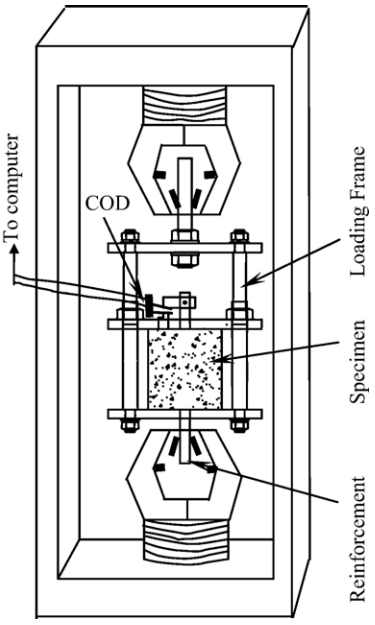

Fig. 2. Test setup.

corroding, thereby representing an average corrosion level along the bond length; see Eq. (2). The actual corrosion level was determined with the following equation:

$$C_R = \frac{G_0 - G}{g_0 l} \times 100\% \quad (2)$$

where G_0 is the initial weight of the steel bar before corrosion, G the final weight for the steel bar after removal of the corrosion products, g_0 the weight per unit length of the steel bar, and l the bond length.

The pullout tests were performed using a universal testing machine that had a capacity of 50 kN. A specially designed loading frame was used for the tests under pullout loading, as shown in Fig. 2. In order to measure the slip more accurately, one crack opening displacement (COD) gauge was used during loading when the slip was less than 2.0 mm, while a linear variable differential transducer (LVDT) (not shown) was used during the entire loading cycle. The outputs from the COD and the LVDT as well as the loads were connected to a computer. All the loads were applied through the computer, using displacement-control. For all the tests, the maximum strain in the steel bars was less than 30 MPa and yielding of the steel bars was not observed.

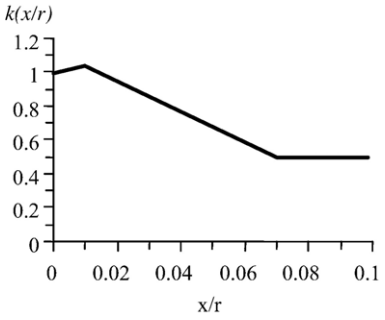

Fig. 4. The chosen function.

3. FE analysis

The modelling method used is specially suited for detailed finite element analyses, where both the concrete and the reinforcement are modelled with solid elements. Special interface elements were used at the surface between the reinforcement bars and the concrete to describe a relation between the traction **t** and the relative displacement **u** in the interface. The physical interpretations of the variables are as described in Eq. (3).

$$\mathbf{t} = \begin{bmatrix} t_n \\ t_t \end{bmatrix} = \begin{bmatrix} \text{normal stress} \\ \text{bond stress} \end{bmatrix} \qquad \mathbf{u} = \begin{bmatrix} u_n \\ u_t \end{bmatrix} = \begin{bmatrix} \text{relative normal displacement} \\ \text{slip} \end{bmatrix} \quad (3)$$

The corrosion model and the bond model developed in [22,26] were used to describe the effect of corrosion and bond. The corrosion model and the bond model can be viewed as two separate layers around a reinforcement bar. However, to reduce the number of nodes required to model a structure, they are integrated in one interface element. Due to equilibrium between the two layers, the traction **t** is the same in the bond

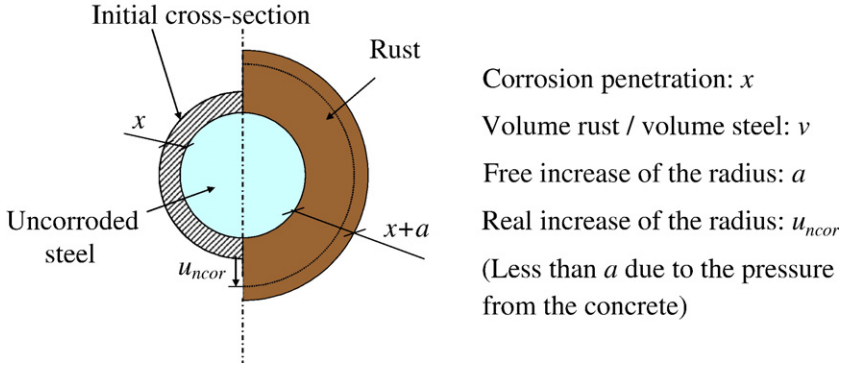

Fig. 3. Physical interpretation of the variables in the corrosion model.

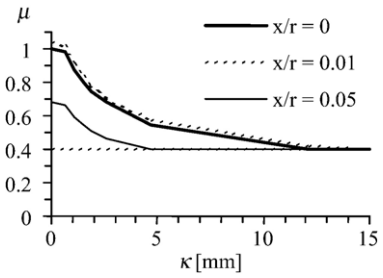

Fig. 5. The resulting function.

and in the corrosion layer. The deformations are related as in Eqs. (4) and (5).

$$u_n = u_{ncor} + u_{nbond} \quad (4)$$

$$u_t = u_{tbond}, \quad u_{tcor} = 0 \quad (5)$$

where the index *cor* means for the corrosion layer, and the index *bond* means for the bond layer.

All input parameters for both the corrosion and the bond model were chosen as described in [22,26]. No adjustments whatsoever was done to fit the results of the experiments described here. The corrosion and bond model are briefly described here, for details see [22,26].

In the corrosion model, the swelling effect of the rust was included, and rust was assumed to behave like a granular material; i.e. its stiffness increased with the stress level. Fig. 3 shows the physical interpretation of the variables in the corrosion model.

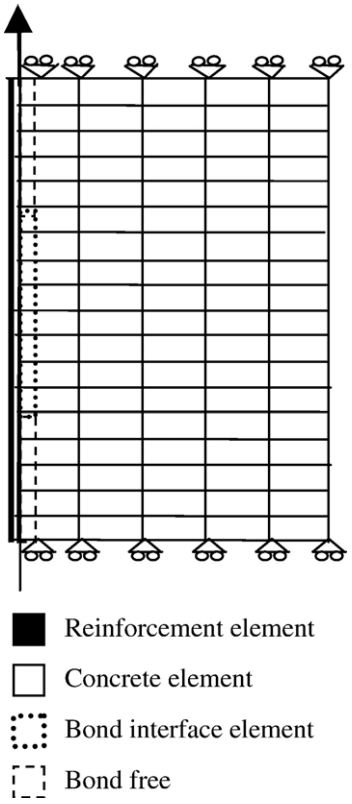

Fig. 6. Mesh for FE analysis of pullout test.

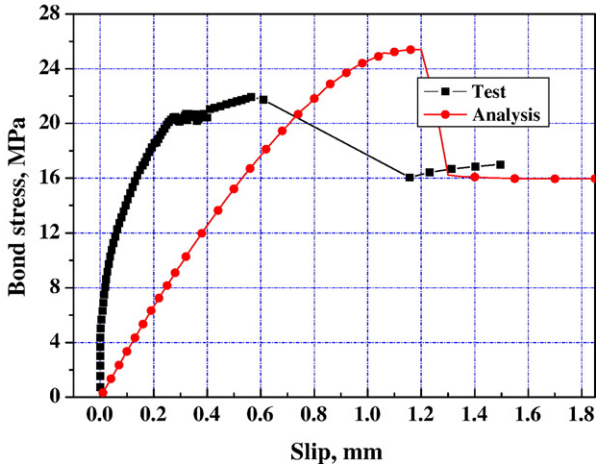

Fig. 7. Bond stress–slip curve in confined non-corroded steel bar.

The volume of the rust relative to the uncorroded steel, and the corrosion penetration as a function of the radius, i.e. how much the radius would increase if the normal stress was zero was calculated from Eq. (6):

$$a = -r + \sqrt{r^2 + (v-1)\cdot(2rx - x^2)} \quad (6)$$

where r is the radius of the reinforcement bar, and the other variables are defined in Fig. 3. The variable v is the volume of the rust relative to the uncorroded steel. This is known to vary depending on what corrosion product that forms. Here, it was assumed to be 2.0, as the other model parameters were calibrated for that value in [26]. It can be noted that the same value was used also in the work of for example [27,28]. The real increase of the radius is u_{ncor}, corresponding to a strain in the rust:

$$\varepsilon_{cor} = \frac{u_{ncor} - a}{x + a} \quad (7)$$

From Eq. (7) strain in the rust, the normal stresses in the layer were determined.

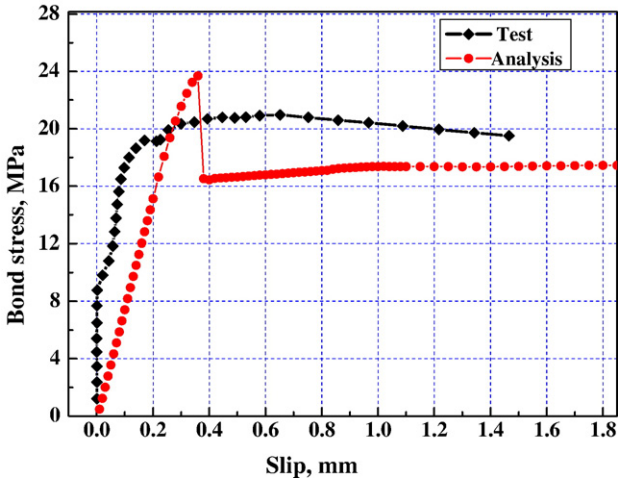

Fig. 8. Bond stress–slip curve in confined steel bar of 3.8% corrosion.

As mentioned before, the corrosion model was combined with a model of the bond mechanism [22]. Corrosion of the reinforcement was assumed to influence the coefficient of friction; for small corrosion penetration, a slight increase in the friction was assumed, while for larger corrosion penetration, the friction was decreased. This was done by introducing a function $k(x/r)$, and letting the coefficient of friction be calculated as in Eq. (8).

$$\mu(\kappa) = k(x/r)\cdot\mu_0(\kappa), \qquad \text{but} \qquad \mu(\kappa)\geq 0.4 \tag{8}$$

where $\mu_0(\kappa)$ is the function chosen for the coefficient of friction for uncorroded reinforcement. The function $k(x/r)$ was chosen as shown in Fig. 4. The resulting function $\mu(\kappa)$ for some corrosion levels are plotted in Fig. 5. The lower limit of the coefficient of friction comes from an assumption that this corresponds to the friction between concrete and concrete. For pullout failure, the failure mode is assumed to be shear cracking between the ribs, and therefore it appears reasonable that the friction at large slips does not depend on the level of corrosion.

The corrosion and bond interface elements were used between solid elements describing the steel and the concrete in the FE analyses. Fig. 6 shows the mesh for FE analysis of the pullout test specimen used in this study. These types of analyses can be done for arbitrary geometries, simply by changing the meshes. Some more examples can be found in [26]. In some examples there, shrinkage of the concrete was included. The concrete was modelled with a constitutive model based on nonlinear fracture mechanics. In analyses using the smeared crack concept, a rotating crack model based on total strain was used. Axisymmetric models were used where four discrete radial cracks were assumed.

4. The results and discussion

Typical tested specimens were modelled, and typical calculation results were compared with the test results. The numerical predictions were generally in reasonably good agreement with the observed maximum bond strengths and stiffnesses of the ascending stage on bond stress–slip curves. Figs. 7–9 show FE analyses compared with the tests for confined bars. It can be noted that there is a discrepancy in stiffnesses for small slips; with less stiffness obtained in the analyses compared to the tests. One reason for this discrepancy can be that the bond model used is mainly calibrated for large slips. Another reason can be that the rib geometry is not exactly similar in these tests as in those the model was calibrated for.

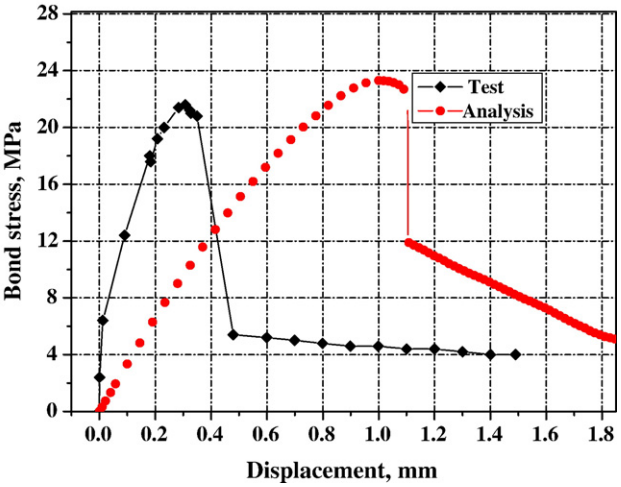

Fig. 10. Bond stress–slip curve in unconfined non-corroded steel bar.

Fig. 7 shows the comparison for confined control specimen (non-corrosion specimen). The maximum bond strength reached was close to the prediction. A sharp drop in bond stress after the maximum value was observed in both prediction and test. The drop in bond stress was caused by cracking in the cover concrete. Fig. 8 shows bond stress–slip curves from FE analysis compared with the tests for a confined bar with a medium corrosion level of 3.8%. The maximum bond strength as well as bond stiffness of the ascending stage of the tests were close to the calculated curve. Larger slip than the control specimen was observed after the maximum bond stress was reached. In Figs. 8 and 7, it can be seen from both experiment and analysis results that the bond strength of the confined steel bar of 3.8% corrosion was only 10% lower than

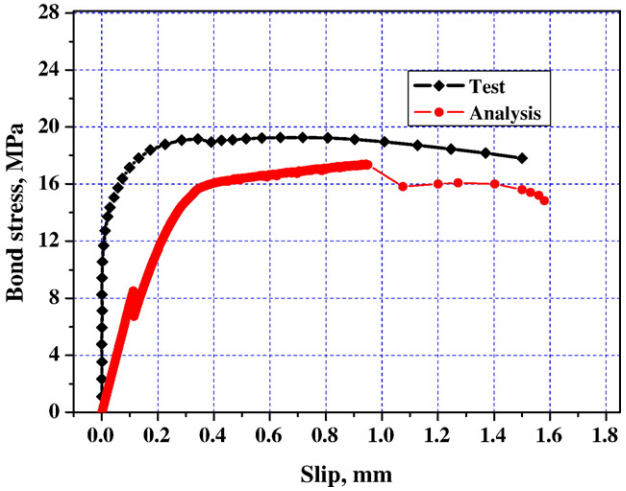

Fig. 9. Bond stress–slip curve in confined steel bar of 6.1% corrosion.

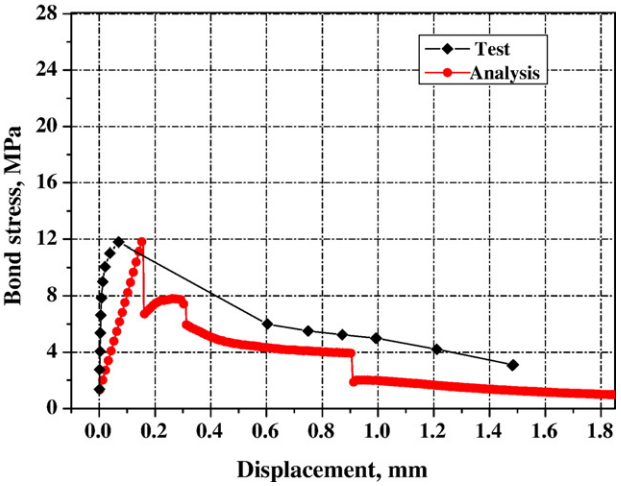

Fig. 11. Bond stress–slip curve in unconfined steel bar of 4.0% corrosion.

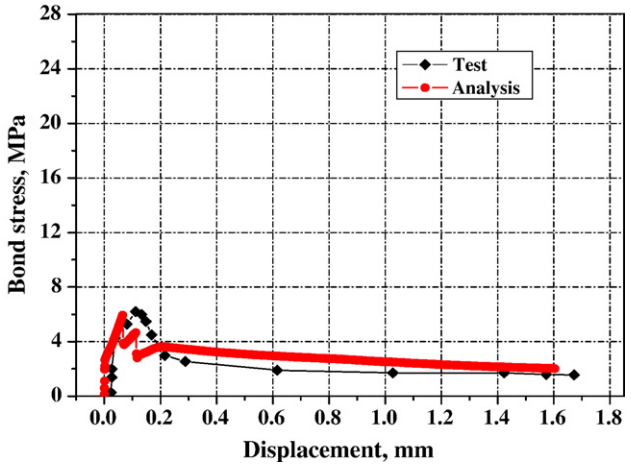

Fig. 12. Bond stress–slip curve in unconfined steel bar of 6.1% corrosion.

that of the confined control specimen (no corrosion). This indicated that for confined deformed bars, corrosion of a medium level (around 4%) had no substantial influence on the bond strength. A possible explanation may be that, for corroded reinforcing steel bars with a low to medium level of corrosion, although corrosion had caused fine cracks in the specimen, the stirrups provided enough confinement. When a pullout load was applied to the specimen, the bearing action of the ribs of the deformed bars against the concrete caused horizontal bearing stresses as well as hoop stresses. Due to the corrosion cracks, the tension in the specimen was reduced and therefore the confinement was reduced and the slip increased which finally resulted in bond failure of the specimen. For the corrosion levels in this range, bond failure usually was the result of splitting of the specimen along the corrosion cracks. For this type of failure, the corrosion-induced cracks had already weakened the concrete.

Fig. 9 shows bond stress–slip curves from FE analysis compared with the tests for a confined bar with a corrosion level of 6.1%. No apparent failure was observed until the slip reached 1.5 mm. This can be considered as a post-peak plateau or residual bond strength.

Figs. 10–12 show bond stress–slip curves from FE analysis compared with the tests for unconfined specimens of a corrosion level of 0% (control specimen), 4.0% and 6.1%, respectively. In Fig. 10, similar to the confined control specimen, a sharp drop in bond stress after the maximum value was also observed in both analysis prediction and experiment. For both experiment and analysis results, the drop in bond stress was caused by splitting in the cover concrete. In Fig. 11, the bond stiffness of both experiment and analysis results was greater than that of control specimen.

In Fig. 10, the bond strengths of the unconfined steel bar of the control specimen (no corrosion), 22 and 23.5 MPa respective of test and analysis, were not substantially lower than that of the confined steel bar of the control specimen (no corrosion), 22 and 25.8 MPa, as shown in Fig. 7. In Fig. 11, the bond strengths of the unconfined steel bar of 4.0% corrosion, 12 MPa from both experiment and analysis, was 30–35% lower than that of confined steel bar with a close corrosion level of 3.8%, as shown in Fig. 8. Also, in Fig. 12, the bond strengths of the unconfined steel bar of 6.1% corrosion, 6–6.3 MPa from analysis and tests, were 65% lower than that of the confined steel bar with the same corrosion level, as shown in Fig. 9. These findings demonstrated that confinement supplied an effective way to counteract bond loss for corroded steel bars of a medium corrosion level (around 4% to 6%). The possible explanation may be: The presence of the normal stress is a condition for transferring bond stress after the chemical adhesion between reinforcing bars and concrete is lost. If the normal stresses are lost, bond stresses cannot be transferred. This occurs if the concrete around the reinforcement bar is penetrated by longitudinal splitting cracks, and if there is no confining reinforcement that can continue to carry the forces. This type of failure is splitting failure. When the concrete surrounding the reinforcement bar is well-confined, it can withstand the normal splitting stresses, and a pullout type failure takes place. Under these conditions, the failure is characterized by shear cracking between the adjacent ribs.

After conducting the pullout text, the specimens were broken and the weight loss due to corrosion of the bond portion of steel bar was determined by cleaning it with Clark's solution (ASTM G1-76). Similarly, the degradation in the rib profile was determined by measuring the rib height before applying the impressed current and after cleaning it with Clark's solution. From the results it was observed that the actual corrosion levels measured as the weight loss of the steel bars were generally lower than the corresponding theoretically estimated ones. The difference between the two indicates that other factors such as the permeability of concrete may had played a role in the corrosion. Surface treatment may also be a factor which had influenced the corrosion [29]. Another factor that may have affected the corrosion is the heterogeneity of the coarse aggregate within the specimen. In the current study, however, these factors were not included in the theoretically estimated corrosion levels when Faraday's Law was used. In the current study, the maximum difference between measured and theoretically estimated corrosion level was 20%. The maximum difference in bond strength between replicate specimens was 22%. Despite the data scatter, reasonably good agreement was achieved between tests and FE analysis results with respect to bond strength and bond failure type. It should be noted that the differences between the theoretically estimated and actually measured corrosion levels had no influence on the conclusions, since only the measured corrosion levels were used for the analyses of the test results.

5. Conclusions

(1) For confined deformed bars, a medium level (around 4%) of corrosion had no substantial influence on the bond strength. But substantial reduction in bond took place when corrosion increased thereafter to a higher level of around 6%.
(2) For non-corrosion bars, the bond strengths of unconfined bars were not significantly lower than that of confined

bars. For corroded bars of a corrosion level of around 4–6%, however, both experiment and analysis results showed that the bond strengths of unconfined steel bars were 30–65% lower than that of confined steel bars of a similar corrosion level. It is thus concluded that confinement supplied an effective way to counteract bond loss for corroded steel bars of a medium corrosion level (around 4% to 6%).

(3) The results of finite element analyses, where it was assumed that rust behaved like a granular material, showed a reasonably good agreement with the experiments regarding maximum bond strength and bond stiffness of the ascending stage on the bond stress–slip curve.

(4) The above findings and conclusions are preliminary, and the first author plans to repeat some of these experiments in future research.

Notation

m_t	theoretically estimated mass loss of reinforcing steel due to corrosion
T	duration of exposure during accelerated corrosion
$\bar{I}$	average current over the duration of exposure which the reinforcement was exposed to
CR	corrosion level
G_0	the initial weight of the reinforcing steel before corrosion
G	the weight of reinforcing steel after removal of the corrosion products
g_0	the weight per unit length of the reinforcing bar
l	bond length
a	free increase of the radius due to corrosion
r	radius of the reinforcing steel
v	volume of rust/uncorroded volume of steel
x	corrosion penetration
ε_{cor}	strain in the rust
u_{cor}	normal deformation in corrosion layer; i.e. increase of the radius due to corrosion
$\mathbf{t}$	traction
$\mathbf{u}$	relative displacement
t_n	normal stress
t_t	bond stress
u_n	relative normal deformation
u_t	slip
u_{ncor}	normal deformation of the corrosion layer when the cover cracks
u_{nbond}	normal deformation in the bond layer
u_{tbond}	slip in the bond layer
u_{tcor}	slip in the corrosion layer
$u(\kappa)$	coefficient of friction
$k(x/r)$	introduced function
$u_0(\kappa)$	function chosen for the coefficient of friction for uncorroded reinforcing steel

Acknowledgements

The first author gratefully acknowledge the support of China State Scholarship and Swedish Institute (SI) Scholarship, which he received for exchange program between the two governments, for a 1-year visit as a guest professor in the Department of Civil and Environmental Engineering, Structural Engineering, at Chalmers University of Technology.

References

[1] M. Maslehuddin, I.M. Allam, G.J. Al-Sulaimani, A.I. Al-Mana, S.N Abduljauwad, Effect of rusting of reinforcing steel on its mechanical properties and bond with concrete, ACI Mater. J. 87 (5) (1990) 496–502.
[2] X. Fu, D.D.L. Chung, Effect of corrosion on the bond between concrete and steel rebar, Cem. Concr. Res. 27 (12) (1997) 1811–1815.
[3] J.G. Cabrera, Deterioration of concrete due to reinforcement steel corrosion, Cem. Concr. Compos. 18 (1996) 47–59.
[4] Y. Auyeung , Bond properties of corroded reinforcement with and without confinement, PhD Thesis, New Brunswick Rutgers, The State University of New Jersey, 2001.
[5] R. Tepfers, A theory of bond applied to overlapped tensile reinforcement splice for deformed bars, Publication, vol. 73:2, Division of Concrete Structures, Chalmers University of Technology, Gothenburg, 1973.
[6] R. Tepfers, Bond stress along lapped reinforcing bars, Mag. Concr. Res. 32 (112) (1980) 135–142.
[7] J. Cairns, K. Jones, The splitting forces generated by bond, Mag. Concr. Res. 47 (171) (1995) 153–165.
[8] J. Cairns, K. Jones, Influence of rib geometry on strength of lapped joints: an experimental and analytical study, Mag. Concr. Res. 47 (172) (1995) 253–262.
[9] G.L. Balázs, Cracking analysis based on slip and bond stress, ACI Mater. J. 90 (4) (1993) 340–348.
[10] A.A. Almusallam, A.S. Al-Gahtani, A.R. Aziz, Rasheeduzzafar, Effect of reinforcement corrosion on bond strength, Constr. Build. Mater. 10 (2) (1996) 123–129.
[11] L. Amleh, S. Mirza, Corrosion influence on bond between steel and concrete, ACI Struct. J. 96 (3) (1999) 415–423.
[12] H.J. Dagher, S. Kulendran, Finite element modeling of corrosion damage in concrete structures, ACI Struct. J. 89 (6) (1992) 699–706.
[13] J. Hou, X. Fu, D.D.L. Chung, Improving both bond strength and corrosion resistance of steel rebar in concrete by water immersion or sand blasting of rebar, Cem. Concr. Res. 27 (5) (1997) 679–684.
[14] S. Ahmad, Reinforcement corrosion in concrete structures, its monitoring and service life prediction – a review, Cem. Concr. Compos. 25 (2003) 459–471.
[15] C. Fang, K. Lundgren, L. Chen, C. Zhu, Effect of corrosion on bond in reinforced concrete, Cem. Concr. Res. 34 (11) (2004) 2159–2167.
[16] R. Capozucca, Damage to reinforced concrete due to reinforcement corrosion, Constr. Build. Mater. 9 (5) (1995) 295–303.
[17] H.S. Lee, T. Noguchi, F. Tomosawa, Evaluation of the bond properties between concrete and reinforcement as a function of the degree of reinforcement corrosion, Cem. Concr. Res. 32 (2002) 1313–1318.
[18] C.K. Soh, S.P. Chiew, Y.X. Dong, Concrete–steel bond under repeated loading, Mag. Concr. Res. 54 (1) (2002) 35–46.
[19] C.K. Kankam, A routine method for measuring bond stress, steel strain and slip in reinforced concrete beams at service loads, Mag. Concr. Res. 55 (1) (2003) 85–93.
[20] M.H. Harajli, B.S. Hamad, A.A. Rteil, Effect of confinement of bond strength between steel bars and concrete, ACI Struct. J. 101 (5) (2004) 595–603.
[21] L.N. Lowes, J.P. Moehle, S. Govindjee, Concrete–steel bond model for use in finite element modeling of reinforced concrete structures, ACI Struct. J. 101 (4) (2004) 501–511.
[22] K. Lundgren, Bond between ribbed bars and concrete: Part 1. Modified model, Mag. Concr. Res. 57 (7) (September 2005) 371–382.
[23] D. Coronelli, Corrosion cracking and bond strength modeling for corroded bars in reinforced concrete, ACI Struct. J. 99 (3) (2002).
[24] M. Berra, A. Castellani, D. Coronelli, S. Zanni, G. Zhang, Steel–concrete bond deterioration due to corrosion: finite-element analysis for different confinement levels, Mag. Concr. Res. 55 (3) (2003) 237–247.
[25] fib (International federation for Structural Concrete), Bond of reinforcement in concrete, State-of-art report prepared by Task Group Bond Models, fib bulletin 10, Lausane, 2000.

[26] K. Lundgren, Bond between ribbed bars and concrete: Part 2. The effect of corrosion, Mag. Concr. Res. 57 (7) (September 2005) 383–396.
[27] D. Coronelli, Bar corrosion in steel–concrete bond: material and structural effects in R/C, PhD. Thesis, Structural Engineering Department, Politecnico di Milano, Milano, 1998.
[28] F.J. Molina, C. Alonso, C. Andrade, Cover cracking as a function of rebar corrosion: Part 2. Numerical model, Mater. Struct. 26 (1993) 532–548.
[29] J. Cairns, C. Melville, The effect of concrete surface treatments on electrical measurements of corrosion activity, Constr. Build. Mater. 17 (2003) 301–309.